THE AMERICAN SOCIETY OF MECHANICAL ENGINEERS
345 E. 47th St., New York, N.Y. 10017

97-GT-150

EFFECT OF FUEL/AIR RATIO ON AIR BLAST SIMPLEX NOZZLE PERFORMANCE

Michael A. Benjamin
Parker Hannifin Corporation
Cleveland, OH 44112-1290

Vincent G. McDonell and G. Scott Samuelsen
University of California at Irvine
Irvine, CA 92697-3550

ABSTRACT

The Air-Blast Simplex (ABS) nozzle may have significant mechanical design advantages when compared to Pure Air-Blast (PAB) designs, and attractive cost benefits. The major barrier to implementing ABS nozzles is spray collapse at high ambient pressures. The present study addresses this issue, and presents the results in a manner that is useful to the gas turbine combustor designer. The results reveal that spray collapse is not significant as long as the fuel-to-air mass ratio is maintained below about 0.3. The results also reveal two distinct curves for air effective area that are attributed to the presence or lack of flow separation in the vane/shroud assembly. In the case of the separated flow, a larger rate of decrease in effective area with increasing fuel air mass or momentum ratio is observed. These results help address ABS spray angle collapse at high pressure, and identify strategies that may adequately mitigate, or even eliminate, spray collapse in a suitably designed combustor.

NOMENCLATURE

AC_d - Air passage effective area (geometric area × flow discharge coefficient)
k - ratio of constant pressure specific heats
P - static pressure downstream of nozzle
P_0 - total pressure upstream of nozzle
T - absolute static temperature downstream of nozzle
T_0 - absolute total temperature upstream of nozzle
V - velocity
w - mass flow rate
ΔP_f - fuel pressure drop across nozzle
ρ - density

subscripts
a - air
f - fuel

INTRODUCTION

The Air Blast Simplex (ABS) nozzle is a twin-fluid air-assist atomizer that uses a pressure-swirl, (simplex) atomizer for liquid delivery while using atomizing air at a relatively low pressure drop ($\Delta P < 6\%$) to aid in the atomization and mixing process. Interest in Air Blast Simplex (ABS) nozzles has recently increased in the aeronautical gas turbine community for at least three reasons:

(1) ABS nozzles are less expensive to manufacture than Pure Air Blast (PAB) atomizers.
(2) the heat shielding around the fuel passages required to inhibit fuel coking, is simpler to design and implement for ABS nozzles than the designs required for the small gaps between the inner and outer air swirlers of a PAB nozzle.
(3) the simplex atomizer has a higher altitude relight capability than a prefilming PAB nozzle for a given low fuel pressure drop. The introduction of the piloted airblast atomizer successfully addressed this last point, yet it suffers from increased complexity and higher cost than the prefilming PAB nozzle.[3]

Figure 1 shows details of the ABS and PAB nozzles used in this study.

A major barrier to implementing ABS nozzles has been the often voiced concern that the simplex atomizer spray collapses at high ambient pressures and is therefore undesirable for

Presented at the International Gas Turbine & Aeroengine Congress & Exhibition
Orlando, Florida — June 2–June 5, 1997

takeoff and climbout in aeronautical applications. However, little information is available regarding how the air-blast and simplex portions of the injector interact, especially at elevated pressures.

While little research has been conducted on air-blast simplex injectors, many studies have been conducted on pure simplex, and pure air-blast atomizers.

Simplex injectors have been studied extensively including the effects of ambient pressure. Parsons and Jasuja[1] examined the spatial distribution of simplex atomizer sprays at several pressures up to 13 atm., and found that the influence of gas pressure (P_a) on the half width (y) of the spray envelope 30 mm downstream of the nozzle face could be adequately described by $y \propto P_a^{-0.25}$. Hiroyasu et. al.[2] made spray distribution measurements up to 69 atm. discharge pressure using a simplex atomizer. They found that the hollow cone spray became a solid spray above 30 atm., but Sauter Mean diameter increased minimally over the whole pressure range. The spray angle was found to decrease from 1 to 30 atm. and then increase above this pressure. However, the angle was always less than that at atmospheric pressure.

Lefebvre[3] cites measurements of radial and circumferential liquid distributions for a number of airblast atomizers. The results showed that increasing the pressure drop across the nozzle caused the peak volume flux measurements on either side of the centerline to move closer together, while the concentration of liquid in the middle of the spray increased. The variation of equivalent spray angle showed a continuous reduction with increasing differential air pressure. An increase in liquid flow rate at low air pressure differential caused the cone angle to first decrease slightly and then increase slightly, while at higher air pressure differential the equivalent spray angle decreases initially and then remains appreciably constant.

Zheng et al.[4] investigated the structure of pure air-blast sprays under ambient pressure conditions of 1, 6 and 12 bar, and flowrates up to 270 kg/h. They found that increasing the ambient pressure at constant fuel-to-air ratio caused the initial spray cone angle to widen from 85° to 105°. Further downstream, the spray volume remained largely unaffected by the ambient pressure.

The studies conducted to date suggest that an important interaction may result from the combination of the air-blast and the simplex. While the simplex spray tends to collapse at elevated pressures, the air-blast tends to be less affected and perhaps even widen. As a result, the present study has been conducted to quantify how the *combined* air-blast and simplex concept behaves at elevated pressures.

EXPERIMENTAL SETUP

The test fluid used for all the experiments was aviation Jet-A. At 25 °C, Jet-A has a density of 799 kg/m^3 and kinematic viscosity of 1.68×10^{-6} m^2/s. To help establish the basic flowfield patterns downstream of the two injectors, a study was conducted at 1 atm with the single phase flow. In this case, a two component laser anemometry system was utilized to quantify the mean and fluctuating axial, radial, and tangential velocity components.

For the 10 atm. experiments, video was utilized to document the behavior of the sprays for all combinations of the conditions shown in Table 1. At higher air flow rates some recirculation of the liquid occasionally impacted the windows. However, averaging 30 individual frames served to reduce the influence of this phenomenon on the conclusions. The averaging was conducted by playing the video segments into a video frame grabber (DT3851-4) and using the video averaging mode of the driver software (Media Cybernetics). The resultant averaged images were then available for additional analysis including spray angle.

Table 1. 10 atm. flow conditions.

Fuel Flow Rates w_f (kg/hr)	Nozzle Air Pressure Drops, (%)
34.0, 47.9, 61.7, 75.6, 89.5, 103, 117, 131, 145, 159	1.5, 3.0, 4.5, 6.0

The results obtained include measurement of the effective area. The effective area is defined from the one-dimensional continuity equation as

$$AC_d = \frac{w_a}{\rho V} \tag{1}$$

To determine the velocity it is required to consider the compressible, one-dimensional conservation equations for continuity and energy, combined with the assumption of a thermally perfect ideal gas and the definition of Mach number. This results in a working equation of

$$AC_d = \frac{\left(\frac{w_a}{P}\right)}{\sqrt{\frac{2k}{(k-1)RT_0}\left(\frac{P_0}{P}\right)^{\frac{k-1}{k}}\left(\left[\frac{P_0}{P}\right]^{\frac{k-1}{k}}-1\right)}} \tag{2}$$

which requires the measurement of the mass flow rate and the pressure drop across the nozzle. The mass flow rate was determined from the pressure drop across a 4.572 mm sonic

venturi fabricated specifically for the purpose of these tests and calibrated against a laminar flow element. Uncertainty in the pressure drop reading was ±1250 Pa.

The fuel-to-air momentum ratio was calculated using the one-dimensional definition of momentum:

$$M = wV \tag{3}$$

This results in the fuel-to-air momentum ratio

$$\frac{M_f}{M_a} = \frac{w_f\sqrt{2\Delta P_f/\rho_f}}{w_a^2/(\rho_a A C_d)} \tag{4}$$

where the fuel velocity is calculated from the Bernoulli equation.

RESULTS AND DISCUSSION

Gas Phase Velocities at 1 atm.

As the ABS nozzle is often benchmarked against the PAB, it is useful to first examine the mean air velocity fields of each with no fuel spray. Figures 2 and 3 compare the mean axial, azimuthal and radial velocity components for the ABS nozzle used in this study with a similar PAB nozzle (see Figure 1). These results were obtained at 1 atm. discharge pressure and with a nominal nozzle pressure drop of 3000 Pa (3.0%). The ABS nozzle had an effective area of 69 mm^2 ± 5% and the PAB nozzle had an effective area of 107 mm^2 ± 5%. The outer swirler and shroud was the same for both nozzles.

It is observed that the general flow field features of the two configurations are very similar. The axial velocity for both nozzles shows that there are recirculation regions in the central region of the near-field that extend to about 30 mm downstream. One difference that can be seen is the slightly longer extent of the zero axial velocity contour (recirculation region) in the center of the ABS flow field. The extent of the flow fields in the radial direction are generally shown by the zero value contours to the far left and right of the centerline, even though there is entrainment from the quiescent air denoted by the radial velocity contour lines outside and upstream of this region for both nozzles. The azimuthal velocity contours show very similar patterns of counter-clockwise rotation with a clearly defined axis along the nozzle centerlines. The difference in the flow fields appears to be negligible at this 3% pressure drop, so one might not expect a significant difference in the spray flow fields at high ambient pressure. However, the tenfold increase in pressure and, hence, momentum and dynamic pressure, can significantly alter the droplet trajectories.

Spray Angle at 10 atm.

Figure 4 shows a typical video image of the ABS nozzle spraying at 10 atm. along with a representation of the spray angle measurement procedure. A line profile was drawn across the image at axial distances corresponding to 1 and 2 swirler outlet diameters. A line was then drawn intersecting the outer edge of the swirler outlet and the location on the line profile at which the intensity value was found to be 20 (out of a maximum of 256). The same process was repeated on both sides of the spray, and the included angle between the two lines is considered to be the spray angle. Note that at the higher air flows, image intensity perturbation due to spray on the windows became more pronounced as adequate screen air flow was not available. This caused the larger scatter in the data at the higher air flows. However, the trend of the cone angle with increasing air flow is consistent.

Figure 5(a) shows spray angle measured 1 diameter downstream of the nozzle as a function of fuel flow and nozzle air pressure drop. At 1.5% pressure drop, the spray cone exhibits a systematic collapse with fuel flow rate exceeding 100 kg/h. Increasing the air flow rate to a level corresponding to a 3% pressure drop delays the collapse with increasing fuel flow rate until 130-140 kg/h. Further increasing the air pressure drop to 4.5% and 6% does not further delay the cone collapse indicating that the spray is "saturated" with air.

Figure 5(b) shows spray angle measured 2 diameters downstream of the nozzle as a function of fuel flow and nozzle air pressure drop. At 1.5% air pressure drop, the spray cone angle behavior is similar to the 1 diameter measurement, except that saturation is reached at a slightly higher fuel flow rate of 120 kg/h. The spray cone angle at 3% air pressure drop does not appear to be fully saturated at the maximum fuel flow rate tested. At the 4.5% and 6% air pressure drops, a change in spray cone angle behavior occurs. At fuel flow rates up to about 75 kg/h, the spray angle increases about 10%. Visually, this corresponds to an overall change in shape of the spray from a straight edge spray to one with an inflection in the near field.

Effective Area

It is important to quantify the fuel air ratio for combustor design and Figure 6 shows the effective areas for the test points. It can be seen that the effective area decrease up to about 10% with increasing fuel flow rate for all but the 1.5% air pressure drop cases. The 1.5% air pressure drop cases appear to have a reduced decrease in effective area with increasing fuel flow rate.

Correlation with Mass and Momentum Ratio

From the above results, it is difficult to draw conclusions about the fuel air mixing at high pressure in the ABS nozzle.

Therefore, the spray angles and effective areas have been plotted against fuel air mass flow ratio and fuel air momentum ratio. Figure 7 shows the results for spray angles plotted against fuel air mass flow ratio at 1 and 2 diameters downstream. Despite the scatter in the data, it is clear that the dependency of spray angle on air pressure drop has been eliminated. The curve for 1 diameter downstream monotonically decreases to a minimum value of about 30° at a fuel air ratio greater than 1. The curve for 2 diameters downstream has a maximum spray angle of nearly 70° at a fuel air ratio of 0.2 and then decreases monotonically to a minimum value of about 30° at a fuel air ratio greater than 1. This decrease is similar to that for 1 diameter downstream and corresponds to the fuel air ratio regime in which a straight edge spray is formed. For fuel air ratios of less than 0.25, a spray is formed that has a larger spray angle at 1 diameter downstream than that at two diameters downstream of the nozzle exit. This suggests that the air is entrained into the center of the spray differently at fuel air ratios less than 0.25 than greater than 0.25.

Figure 8 shows plots of spray angle at 1 and 2 diameters downstream plotted against fuel air momentum ratio. Again, all the data collapses onto single curves and show the same spray shape effects as the fuel air mass ratio results.

Effective area is plotted against fuel air mass and momentum ratios in Figures 9(a) and (b), respectively. The 1.5% air pressure drop data falls onto a different curve than the data at the three higher pressure drops. Secondly, at 3.0% pressure drop, a local minimum in effective area is observed. Thirdly, the rate of decrease in effective area is significantly less for the 1.5% pressure drop cases than for the higher pressure drop data. A fourth effect is seen for the higher pressure drop cases in Figure 9(b). At fuel air momentum ratios above about 6, the rate of decrease in effective area returns to about the same rate of decrease as for the 1.5% pressure drop case. Micklow and Benjamin[5] computed air flows in this same overall geometry, but with a less severe turning air swirler, and found that a separation bubble forms on the vanes at a 3% pressure drop. Also, it extended beyond the vane trailing edges into the shroud flow. It is therefore suspected that separation from the swirler vanes is the cause of the increased rate of effective area decrease that occurs between 1.5% and 3% air pressure drop. The decreased reduction in effective area at the higher fuel air momentum may correspond to a fully separated condition.

SUMMARY AND CONCLUSIONS

A study to examine the discharge coefficient and spray angle of an air-blast simplex (ABS) nozzle operating in an ambient pressure of 10 atm has been conducted. The objective of the study was to examine possible regimes which will preclude spray collapse at high ambient pressures thereby allowing the cost and mechanical design advantages of the ABS nozzle relative to the pure air-blast design to be implemented. Conclusions drawn are as follows:

- Spray angle correlates with momentum and mass ratio independent of pressure drops from 1.5 to 6%.
- The injector effective area correlates with the mass and momentum ratio but reveals two independent regimes that are associated with either presence or absence of flow separation behind the swirl vanes.
- At pressure drops above 3%, effective area decreased with increase fuel-to-air mass ratio or momentum ratio.
- At pressure drops of 1.5%, effective area was independent of fuel-to-air mass or momentum ratio.
- At fuel-to-air mass ratios below 0.3, effective area and spray angle were found to be independent of pressure drop implying that if mass ratios are maintained below this value, the spray collapse can be avoided.

ACKNOWLEDGMENTS

The authors would like to thank the Parker Hannifin Corporation, Gas Turbine Fuel Systems Division, for permission to publish this paper. Also, we would like to acknowledge the contribution of Mr. Bob Pelletier of Parker Hannifin for some of the initial work on this topic. The experiments were conducted at the UCI Combustion Laboratory, University of California, Irvine. The assistance of Mr. Jason Campbell and Mr. Steven Lee in the operation of the facility and acquisition and reduction of the data is appreciated.

REFERENCES

1. Parsons, J. A., 1986, "Effect of Air Pressure Upon Spray Angle/Width Characteristics of Simplex Pressure Swirl Atomizers," Int. J. Turbo and Jet Engines, Vol. 3, pp. 207-216.
2. Hiroyasu, H., Arai, M., and Atarashiya, K., "Spray Characteristics of Swirl Atomizer at Pressurized Conditions," Proceedings of the 1987 Tokyo International Gas Turbine Conference, Vol. 3, pp. 69-76.
3. Lefebvre, A. H., 1979, Atomization and Sprays, Hemisphere Publishing Corporation, New York.
4. Zheng, Q. P., Jasuja, A. K., and Lefebvre, A. H., 1996, "Structure of Airblast Sprays under High Ambient Pressure Conditions," 96-GT-131, ASME International Gas Turbine and Aeroengine Congress & Exhibition, Birmingham, U. K.
5. Micklow G., and Benjamin, M. A., 1996, "Three-Dimensional Analysis of Advanced Swirl Vane/Nozzle Assemblies," 96-GT-226, ASME International Gas Turbine and Aeroengine Congress & Exhibition, Birmingham, U. K.

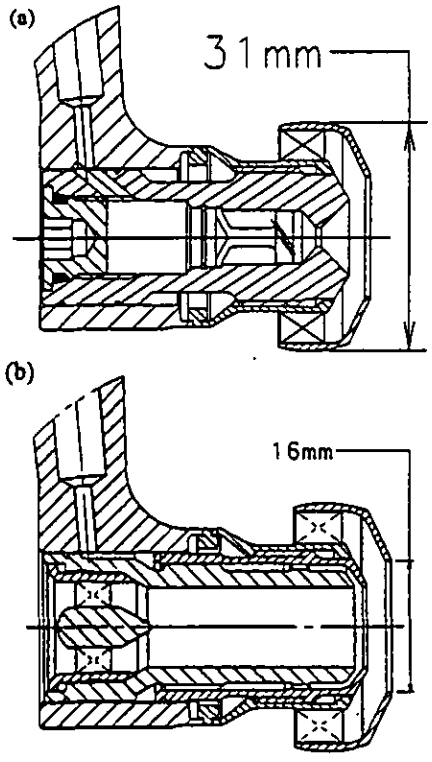

Figure 1. Cross sections of the (a) Air-Blast Simplex (ABS), and (b) Pure Air-Blast (PAB) nozzles used in this study.

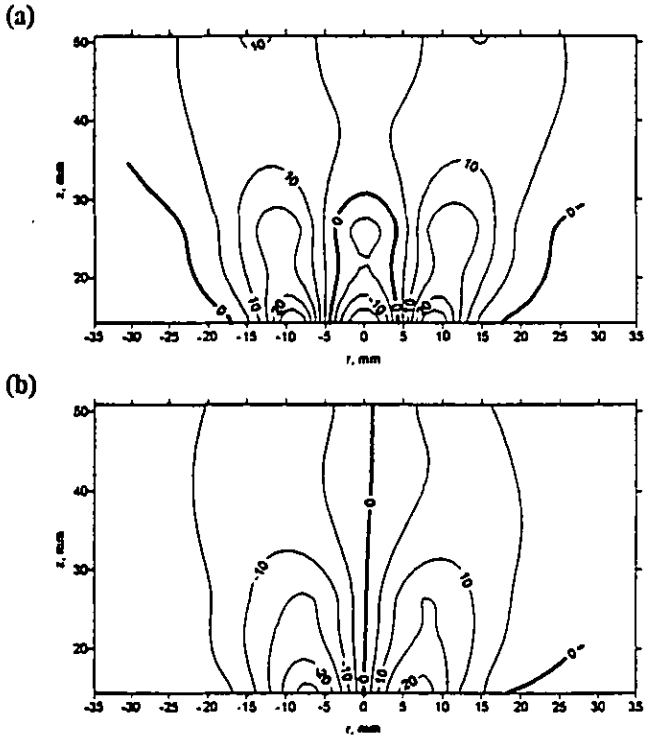

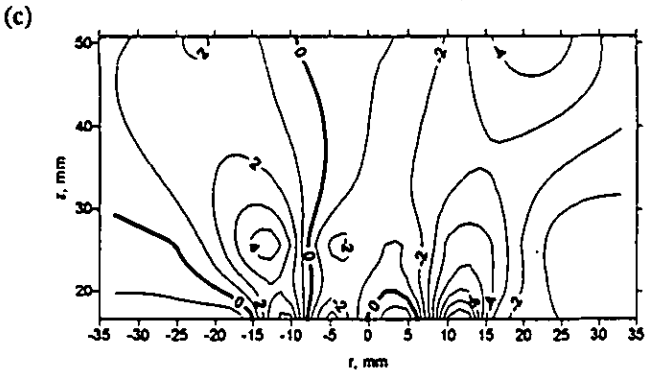

Figure 2. Air-Blast Simplex (ABS) Velocity Contours (m/s): (a) axial, (b) azimuthal, and (c) radial.

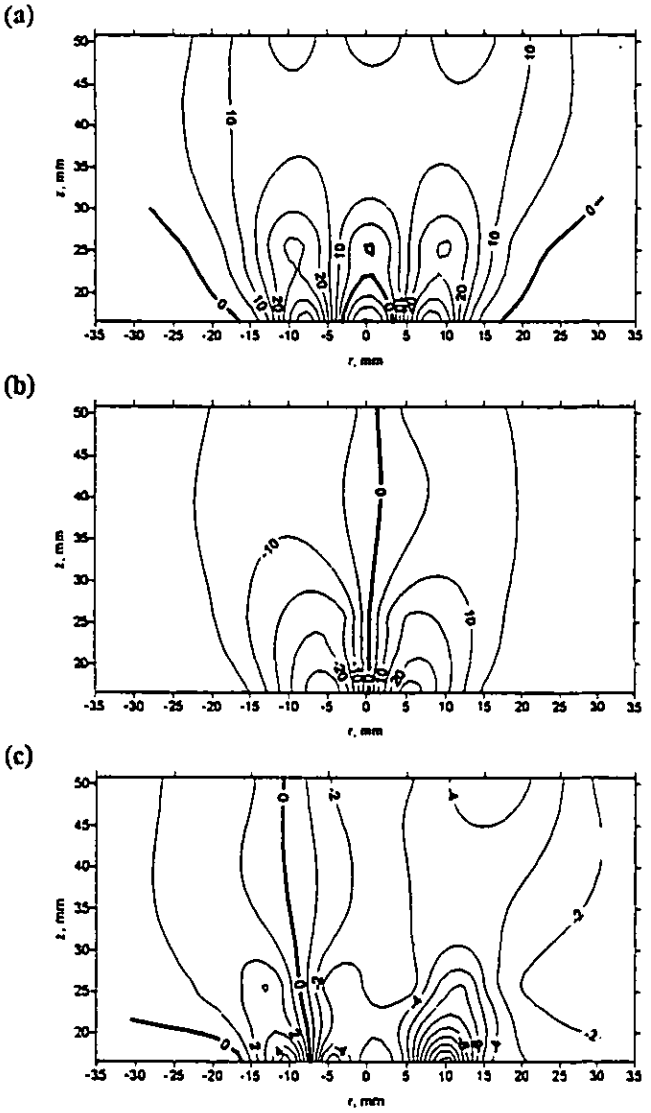

Figure 3. Pure Air-Blast Velocity (PAB) Contours (m/s): (a) axial, (b) azimuthal, and (c) radial.

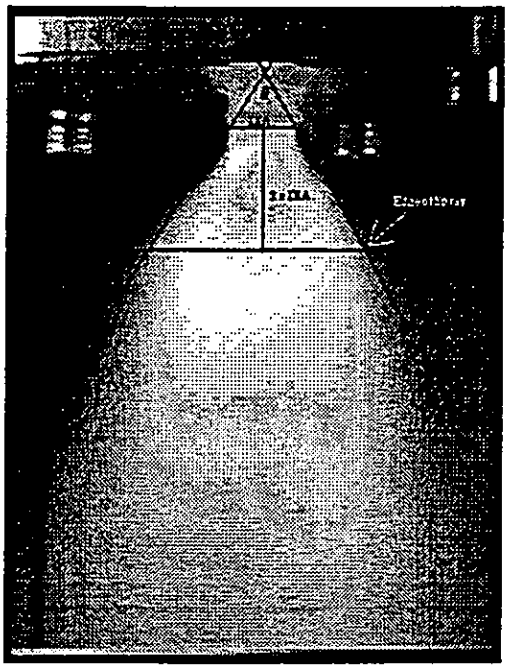

Figure 4. Typical CCD picture showing spray angle measurement technique at two diameters downstream from nozzle shroud.

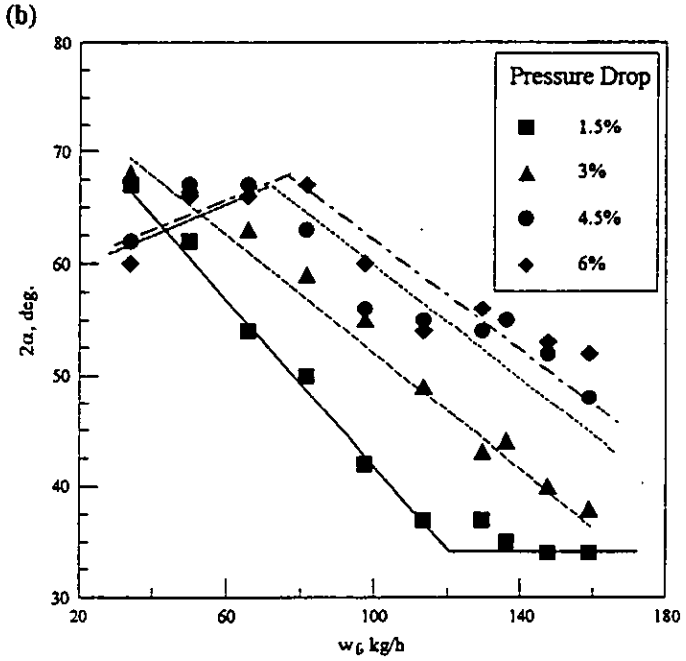

Figure 5. Spray angle measured as a function of fuel flow and nozzle air pressure drop at 10 atm. air pressure: (a) *one* diameter, and (b) *two* diameters downstream of the nozzle.

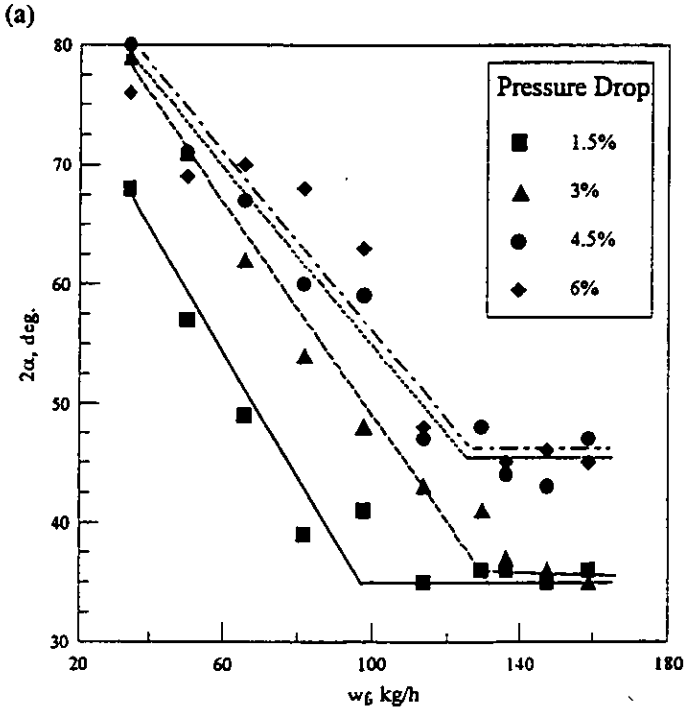

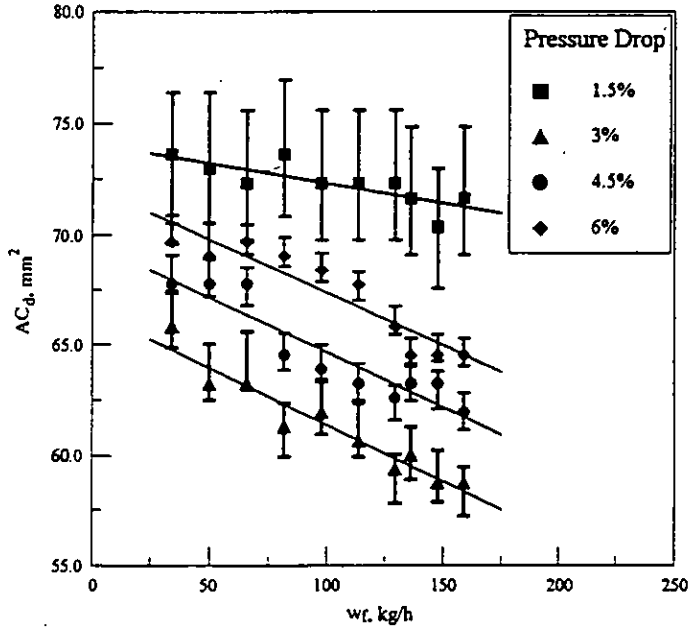

Figure 6. Effective area of the swirler as a function of fuel flow and nozzle air pressure drop at 10 atm. air pressure.

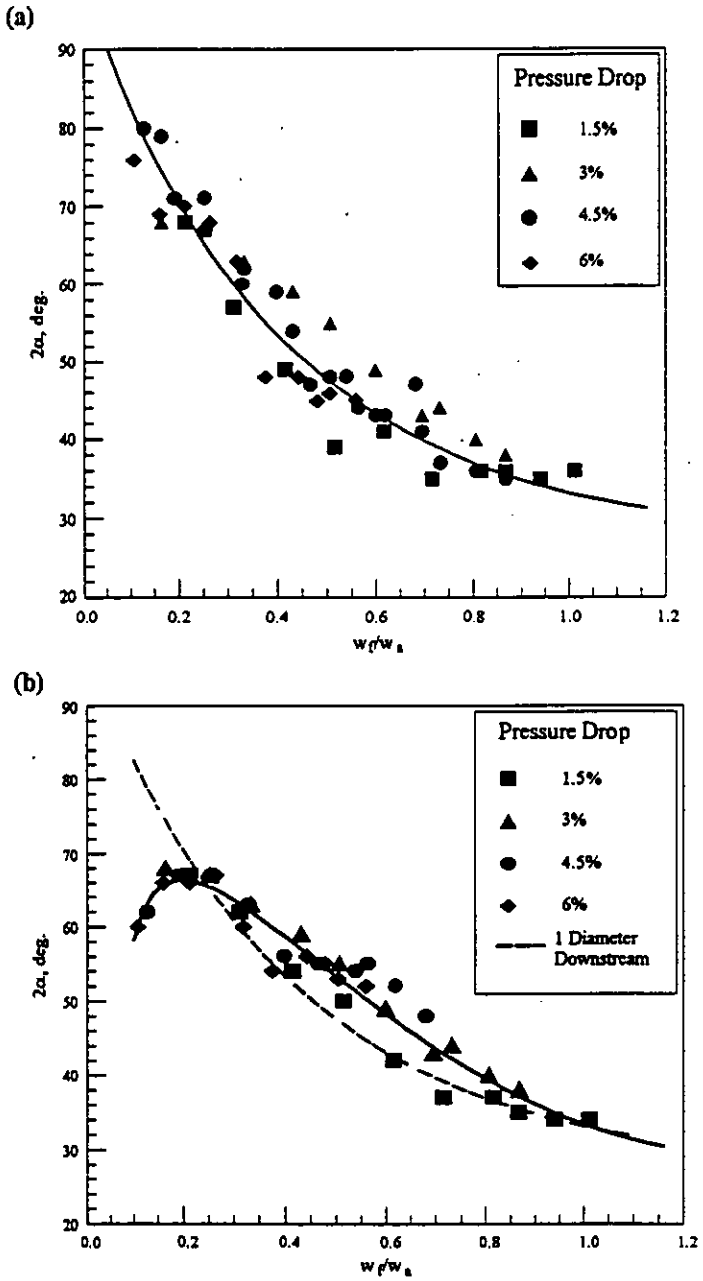

Figure 7. Spray angle measured downstream of the nozzle as a function of nozzle fuel/air ratio and nozzle air pressure drop at 10 atm. air pressure: (a) *one* diameter, and (b) *two* diameters downstream of the nozzle.

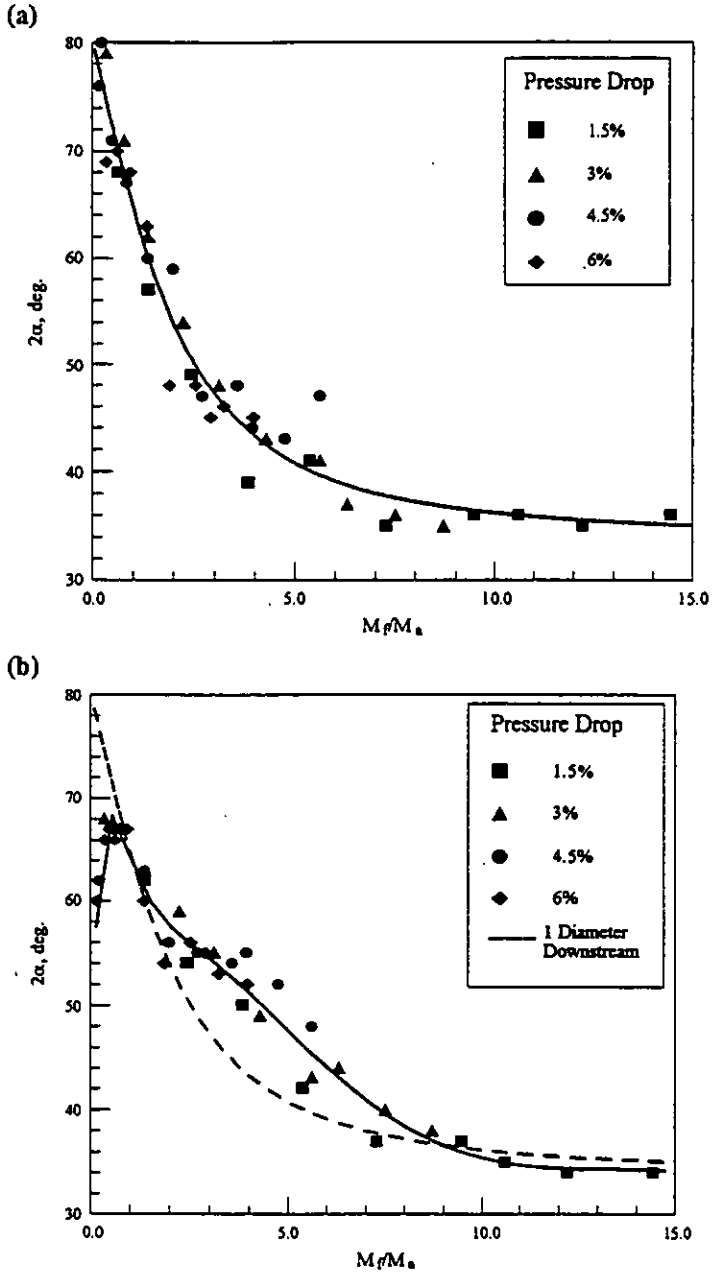

Figure 8. Spray angle measured downstream of the nozzle as a function of nozzle fuel/air momentum ratio and nozzle air pressure drop at 10 atm. air pressure: (a) *one* diameter, and (b) *two* diameters downstream of the nozzle.

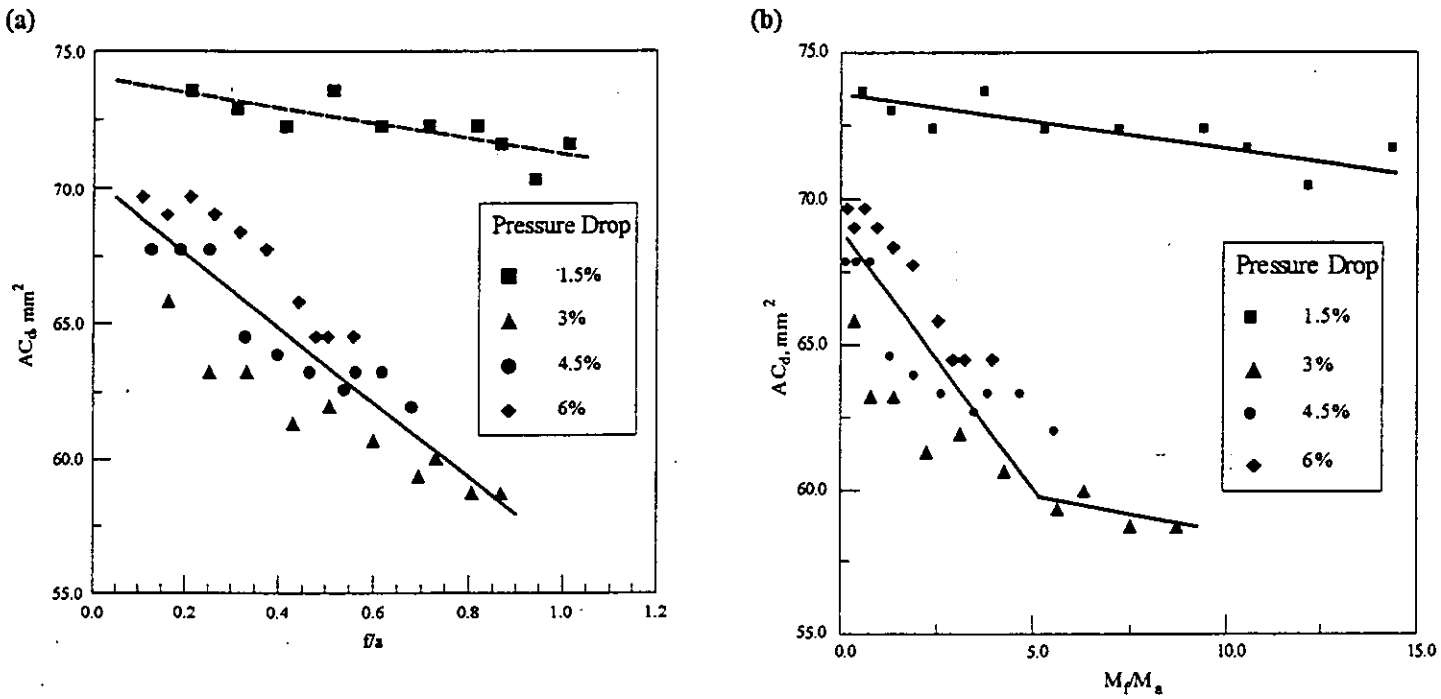

Figure 9. **Effective area of the swirler as a function of nozzle air pressure drop at 10 atm. air pressure and: (a) nozzle fuel/air mass ratio, and (b) nozzle fuel/air momentum ratio.**